molecular pharmaceutics

pubs.acs.org/molecularpharmaceutics

Article

Enhanced Oral Bioavailability of Rivaroxaban-Loaded Microspheres by Optimizing the Polymer and Surfactant Based on Molecular Interaction Mechanisms

Min-Jong Choi,[#] Mi Ran Woo,[#] Kyungho Baek, Ji Hun Park, Seewon Joung, Yong Seok Choi, Han-Gon Choi,* and Sung Giu Jin*

Cite This: *Mol. Pharmaceutics* 2023, 20, 4153−4164

Read Online

ABSTRACT: This study aimed to develop microspheres using water-soluble carriers and surfactants to improve the solubility, dissolution, and oral bioavailability of rivaroxaban (RXB). RXB-loaded microspheres with optimal carrier (poly(vinylpyrrolidone) K30, PVP) and surfactant (sodium lauryl sulfate (SLS)) ratios were prepared. ^{1}H NMR and Fourier transform infrared (FTIR) analyses showed that drug−excipient and excipient−excipient interactions affected RXB solubility, dissolution, and oral absorption. Therefore, molecular interactions between RXB, PVP, and SLS played an important role in improving RXB solubility, dissolution, and oral bioavailability. Formulations IV and VIII, containing optimized RXB/PVP/SLS ratios (1:0.25:2 and 1:1:2, w/w/w), had significantly improved solubility by approximately 160- and 86-fold, respectively, compared to RXB powder, with the final dissolution rates improved by approximately 4.5- and 3.4-fold, respectively, compared to those of RXB powder at 120 min. Moreover, the oral bioavailability of RXB was improved by 2.4- and 1.7-fold, respectively, compared to that of RXB powder. Formulation IV showed the highest improvement in oral bioavailability compared to RXB powder (AUC, 2400.8 ± 237.1 vs 1002.0 ± 82.3 h·ng/mL). Finally, the microspheres developed in this study successfully improved the solubility, dissolution rate, and bioavailability of RXB, suggesting that formulation optimization with the optimal drug-to-excipient ratio can lead to successful formulation development.

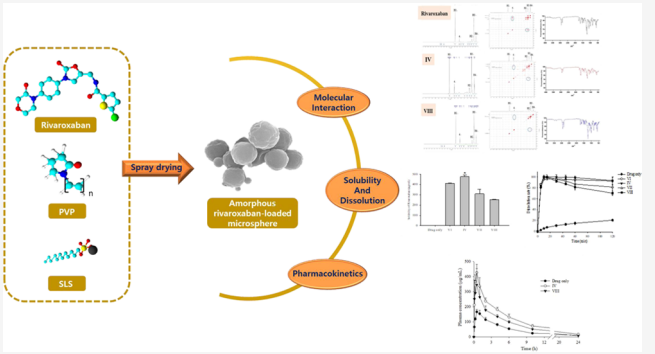

KEYWORDS: *rivaroxaban, microsphere, poorly water-soluble drugs, molecular interaction, oral bioavailability*

1. INTRODUCTION

Thromboembolic disorders are diseases that lead to severe cardiovascular complications and high mortality rates.[1] Rivaroxaban (RXB) is a direct factor Xa (FXa) inhibitor used for the prevention of deep vein thrombosis, acute pulmonary embolism, and venous thromboembolism.[2,3] Direct thrombin inhibitors are more effective than conventional anticoagulants, and they act not only by inhibiting FXa but also via selective inhibition of prothrombinase activity and fibrin-associated FXa activity.[1,2] RXB can also prevent embolic stroke and has been proven to be as safe and effective as warfarin.[3] However, according to the Biopharmaceutical Classification System (BCS), RXB is a class II drug with low oral bioavailability due to high gastrointestinal permeability and low water solubility.[4] Therefore, our goal was to develop a formulation that improves the aqueous solubility of RXB, a poorly soluble anticoagulant, and ultimately enhance its oral bioavailability.

Various formulation strategies have been used to overcome the poor aqueous solubility of RXB, including co-crystallization,[5] self-microemulsifying drug delivery systems,[6] micronization,[4] cyclodextrin inclusion,[7] micelle solubilization,[1] solid dispersion,[4,8] and encapsulation in nanoparticles.[9] Among the various solubilizing techniques available to increase solubility and dissolution, solid dispersion is commonly used to enhance the aqueous solubility, dissolution, and oral bioavailability of RXB, a poorly water-soluble drug.[3,10] Solid dispersion is generally used for a group of solid products, such as hydrophobic drugs, consisting of a hydrophilic matrix and two or more other components.[11] Amorphous solid dispersion

Received: April 5, 2023
Revised: June 27, 2023
Accepted: June 28, 2023
Published: July 11, 2023

https://doi.org/10.1021/acs.molpharmaceut.3c00281
Mol. Pharmaceutics 2023, 20, 4153−4164

Table 1. Compositions of RXB-Loaded Polymeric Microspheres

constituents (g)	I	II	III	IV	V	VI	VII	VIII
rivaroxaban	1	1	1	1	1	1	1	1
PVP	0.25	0.25	0.25	0.25	0.25	0.05	0.5	1
SLS		0.5	1	2	4	2	2	2

is a promising strategy to improve the solubility and bioavailability of poorly soluble drugs. Despite these advantages, amorphous solid dispersion leads to thermodynamic instability, nucleation, and crystal growth, which reduce the drug performance.[12] In this case, an inert polymer called a carrier can be used to reduce intermolecular interactions, nucleation, and crystallization for maintaining a supersaturated state and inhibiting precipitation during dissolution in vivo.[13]

The selection of appropriate excipients to enhance the solubility and oral bioavailability of water-insoluble drugs is important for formulation design. In this study, poly(vinylpyrrolidone) K30 (PVP) and sodium lauryl sulfate (SLS) were used as hydrophilic carriers and surfactants, respectively, with the highest ability to solubilize RXB in a solid dispersion system. PVP is a nontoxic hydrophilic polymer commonly used in pharmaceuticals. It has excellent solubility in solvents of different polarities and good binding properties and has been widely used to enhance the solubility and bioavailability of poorly water-soluble drugs.[14,15] SLS is an anionic surfactant with high solubilizing ability.[16] It is a common solubilizing agent in pharmaceuticals and is generally used as an excipient in oral formulations to improve the aqueous solubility of poorly water-soluble drugs.[7,8,14] Therefore, the combined use of PVP and SLS is expected to enhance the solubilization and dissolution of poorly water-soluble drugs. In this study, we observed an approximately 160-fold increase in the solubility of RXB-loaded microspheres compared with that of the drug powder because of the synergistic effect of the PVP/SLS complex. In addition, to investigate the synergistic effect of the PVP/SLS complex, we investigated the effect of the drug−excipient ratio of the RXB-loaded microspheres on their solubility, dissolution, intermolecular interactions, and oral bioavailability.[4,17] In most solid dispersions, the solubility, dissolution rate, and bioavailability of poorly soluble drugs increased as the amount of excipients, such as polymers and surfactants, increased.[18−20] However, in this study, the solubility and dissolution rate of RXB were higher in the presence of a small amount of polymer (PVP) in the formulation. This was confirmed by a significant decrease in the solubility, dissolution rate, and bioavailability of RXB as the amount of PVP increased in the same SLS-containing formulation. These results confirmed that the drug−excipient ratio influenced the solubility, dissolution, intermolecular interaction, and oral bioavailability of RXB in microspheres.[21]

The present study aimed to develop RXB-loaded polymeric microspheres to improve aqueous solubility and oral bioavailability. There have been several solubilization studies in which the solubility and oral bioavailability of poorly soluble drugs increases as the amount of carriers increases.[4,8] However, this study investigated the interaction of the drug with the carrier and evaluated their effects on physicochemical properties, solubility and oral bioavailability. Unlike previous studies, it was confirmed that the optimal ratio exists depending on the interaction between the drug and the carrier. This could be a promising new strategy for formulation design.

2. MATERIALS AND METHODS

2.1. Materials. RXB, sodium carboxymethyl cellulose, dextran, and SLS were obtained from Hanmi Pharm. Co. (Suwon, South Korea). Polysorbates (Tween 20 and Tween 80) were purchased from Daejung Chem. Co. (Siheung, South Korea). Hydroxypropyl methylcellulose (HPMC 2910, 4, and 6 cps) and Klucel hydroxypropyl cellulose were obtained from Shin-Etsu. Co. (Tokyo, Japan). Cremophor (EL and RH40), PVP, and Poloxamer 407 were purchased from BASF (Ludwigshafen, Germany). Transcutol P, Labrafil (M1944CS), and Labrasol were purchased from Gattefossé (Saint-Priest, France). All other organic solvents used were of analytical reagent grade.

2.2. Analytical Method. High-performance liquid chromatography (HPLC) analysis of RXB was performed using an Agilent 1260 Infinity system (Agilent Technologies, Santa Clara, CA) equipped with an ultraviolet (UV) detector (G1311C 1260 Quat Pump and G1314B 1260 VWD VL detector). The amount of RXB in the sample was determined by reverse-phase HPLC. The analytical column used was a C_{18} column (4.6 × 150 mm^2, 5 μm; Shiseido Capcell Pak MG, Shiseido, Japan), and the mobile phase was composed of acetonitrile and 20 mM ammonium acetate buffer solution adjusted to pH 4.3 (65:35, v/v).[22] The column temperature was set at 35 °C. The injection volume was 20 μL. The flow rate was 1 mL/min with isocratic elution. UV absorbance was maintained at 250 nm.[23] The calibration curve had a linear correlation coefficient of 0.9999 at RXB concentrations of 0.9 to 100.0 μg/mL, confirming that the selected analytical method was linear. All analyses were repeated thrice.

2.3. Preparation and Optimization of RXB-Loaded Microspheres. *2.3.1. Screening of Proper Carriers.* To select suitable carriers for the preparation and optimization of RXB-loaded microspheres, the aqueous solubility of RXB has been investigated in distilled water for various carriers, such as hydrophilic polymers and surfactants.[24] An excess of drug was added to 1 mL of 1% (w/v) polymer and 10% (w/v) surfactant aqueous solution using a method established in previous studies, and the samples were then vortexed for 10 min and placed in an isothermal water bath shaker for 7 days at 25 °C to investigate the maximum solubilization.[25] Afterward, the samples were centrifuged at 10,000*g* for 15 min to separate the undissolved drug and then filtered through a 0.45 μm nylon filter. The supernatant was diluted with dimethyl sulfoxide (DMSO).[24,27] The aqueous solubility of RXB was quantified using HPLC as described above. All experiments were performed in triplicate.

2.3.2. Preparation of RXB-Loaded Microspheres. Based on the aqueous solubility test, the polymer and surfactant with the highest drug solubility were chosen.[19] RXB-loaded microspheres were prepared in various proportions by mixing the drugs, selected polymers, and surfactants in a mixture of acetonitrile/water.[22] Eight different formulations were prepared using the solvent-evaporated solid dispersion method, as shown in Table 1. The drug and the selected polymer and surfactant were stirred until completely dissolved in 2.5 L of a

https://doi.org/10.1021/acs.molpharmaceut.3c00281
Mol. Pharmaceutics 2023, 20, 4153−4164

mixture of acetonitrile/water (40:60, v/v). The resulting clear solution was spray-dried using a laboratory-scale Büchi nozzle-type mini spray dryer (Flawil, Switzerland) to prepare RXB-loaded microspheres. The inlet temperature and outlet temperature were 140 and 90−95 °C, respectively. Using a peristaltic pump, the solution was moved to the nozzle (diameter 0.7 mm) and then sprayed under the following conditions: liquid feed rate, 5.4 mL/min; aspirator, 100%; air spray pressure, 4 kg/cm^2.

2.4. Evaluation of RXB-Loaded Microspheres. *2.4.1. Solubility Studies.* For solubility test of the RXB-loaded microspheres, an excess amount of each sample (equivalent to 1 mg of RXB) was added to 1 mL of distilled water in a 2 mL Eppendorf tube, vortexed, shaken in a water bath (Daihan Scientific, Wonju, South Korea) at 25 °C for 3 days, and centrifuged at 10,000*g* for 10 min (Smart 15; Hanil Science Industrial Co., Gangneung, South Korea).[26] The supernatant was then filtered through a nylon filter (0.45 μm). The filtered samples were diluted with DMSO to quantify RXB using HPLC, as described in Section 2.2.

2.4.2. Drug Content. Drug content was determined by dissolving an accurately weighed amount of each sample (equivalent to 10 mg of RXB) in 100 mL of acetonitrile. The drug content was obtained using the equation $[C_a/C_t \times 100]$, where C_t and C_a are the theoretical and actual drug concentrations, respectively.[24] The solution was filtered through a 0.45 μm membrane and then analyzed using an HPLC system. All experiments were performed in triplicate.

2.4.3. Dissolution Test. The dissolution study of the drug powder (10 mg) and RXB-loaded microspheres (equivalent to 10 mg of RXB) was conducted using USP Apparatus II (the paddle method). The prepared samples were investigated using a dissolution tester (Vision Classic 6; Hanson Research Co., Chatsworth, CA) filled with 900 mL of distilled water. The paddle speed and temperature were maintained at 50 rpm and 37 ± 0.5 °C, respectively. The dissolution medium (3 mL) was collected at several time points (5, 10, 15, 30, 45, 60, and 120 min) and then filtered through a nylon filter (0.45 μm). The drug concentration in the medium was analyzed using HPLC, as described above. All experiments were performed in triplicate.

2.5. Physicochemical Properties of RXB-Loaded Microspheres. *2.5.1. Scanning Electron Microscopy.* The morphologies of the RXB powder and microsphere samples were determined using a scanning electron microscope (S-4800; Hitachi, Tokyo, Japan). The prepared samples were mounted onto a scanning electron microscopy sample stub using a transparent adhesive material. All samples were coated with platinum using a sputter-coating machine (EMI Tech K575K; Emitech Ltd, U.K.) to make them electrically conductive before analysis.

2.5.2. Differential Scanning Calorimetric (DSC) Studies. The thermal aspect of RXB powder and RXB-loaded microspheres was investigated using DSC Q200 (TA Instruments, New Castle, DE). Typically, approximately 3−5 mg of sample was weighed into an aluminum pan, and the operating temperature of the DSC instrument was increased from 50 to 300 °C at a rate of 10 °C /min using nitrogen as the purge gas. The differential scanning calorimetry baseline, temperature, and enthalpy were calibrated using a standard aluminum pan.

2.5.3. Powder X-ray Diffraction (PXRD). PXRD analysis was conducted using an X-ray diffractometer (D/MAX-2500; Rigaku, Japan). The samples, which included RXB powder and RXB-loaded microspheres, were analyzed by exposure to monochromatic Cu Kα radiation (γ = 1.54178 Å) at 100 mA current and 40 kV generator voltage over a range of 2θ angles from 3 to 50° with an angular increment of 0.02°/s. A high-purity Si standard was used for PXRD calibration.

2.5.4. Particle Size Analysis. A Mastersizer 3000 laser diffraction analyzer (Malvern, Worcestershire, U.K.) was used to investigate the particle sizes of the drug and microsphere formulations. All samples were measured under the following conditions: air pressure for dispersion, 1.5 bar; feed rate, 50%; and hopper gap, 1.5 mm. Each powder sample was analyzed in triplicate. The particle size distributions were expressed as D10, D50, and D90, which are the 10th, 50th, and 90th percentiles of the cumulative volume distribution, respectively.[28]

2.5.5. Nuclear Magnetic Resonance (NMR). The 1D ^{1}H NMR and two-dimensional nuclear overhauser effect spectroscopy (2D-NOESY) spectra of RXB/PVP/SLS physical mixture and selected RXB-loaded microspheres (Formulation IV and VIII) were investigated at 500 MHz on a JEOL ECZ 500R spectroscopy (JEOL, Tokyo, Japan) at 25 °C. All samples were diluted in deuterated dimethyl sulfoxide-d6 (DMSO-d6) and transferred to NMR tubes (ϕ = 5 mm) for analysis.[29] The chemical shift changes ($\Delta\delta$) were reported in parts per million (ppm) using tetramethylsilane (TMS) as an external reference.

2.5.6. Fourier Transform Infrared (FTIR) Spectroscopy. The FTIR spectra of the RXB/PVP/SLS physical mixture and selected RXB-loaded microsphere formulations (IV and VIII) were determined at 450 to 4000 cm^{-1} using an FTIR spectrophotometer (Frontier; PerkinElmer, Waltham, MA).[24]

2.6. Pharmacokinetic Studies of RXB-Loaded Microspheres. *2.6.1. Pharmacokinetic Studies.* Male Sprague−Dawley rats (9 weeks old, 300 ± 20 g) were provided by Orient Bio (Sungnam, South Korea). The pharmacokinetic studies were conducted in accordance with the NIH Policy, and the protocols were conducted in accordance with the Institutional Animal Care and Use Committee (IACUC) at Hanyang University. Before the pharmacokinetic experiments, all rats were fasted overnight and kept in an animal cage at 25−27 °C and 55 ± 5% relative humidity.[19] Eighteen rats were randomly divided into three groups of six each, which were orally administered 0.5% CMC-Na suspension liquid of RXB powder (10 mg/kg) and RXB-loaded microspheres dissolved in 1 mL of distilled water (equivalent to 10 mg/kg RXB).[30] Blood samples (0.35 mL) were obtained from the femoral artery at specific time points of 0.083, 0.25, 0.5, 1, 2, 4, 6, 12, and 24 h, collected in heparin-coated microcentrifuge tubes, and centrifuged at 20,000 rpm for 15 min. Next, the plasma (supernatant) was transferred to the labeled tubes and stored at −20 °C for further analysis.[23]

2.6.2. Determination of Rivaroxaban in Rat Plasma. RXB concentrations in rat plasma were quantified according to previously reported techniques using liquid−liquid extraction, liquid chromatography, and multiple reaction monitoring assay (LC-MRM). Apixaban (50 μg/mL in ethyl acetate) was used as an internal standard to ensure analysis of plasma samples.[31] Next, 500 μL of internal standard was added to 20 μL of the plasma sample, followed by mixing for 10 min and centrifugation (15,000 rpm). The supernatant was then dried under a nitrogen stream, and the resulting residue was redissolved in 100 μL of 30% (v/v) aqueous acetonitrile solution and centrifuged (15,000 rpm). Finally, LC-MRM was conducted using the Shimadzu Nexera UPLC System

https://doi.org/10.1021/acs.molpharmaceut.3c00281
Mol. Pharmaceutics 2023, 20, 4153−4164

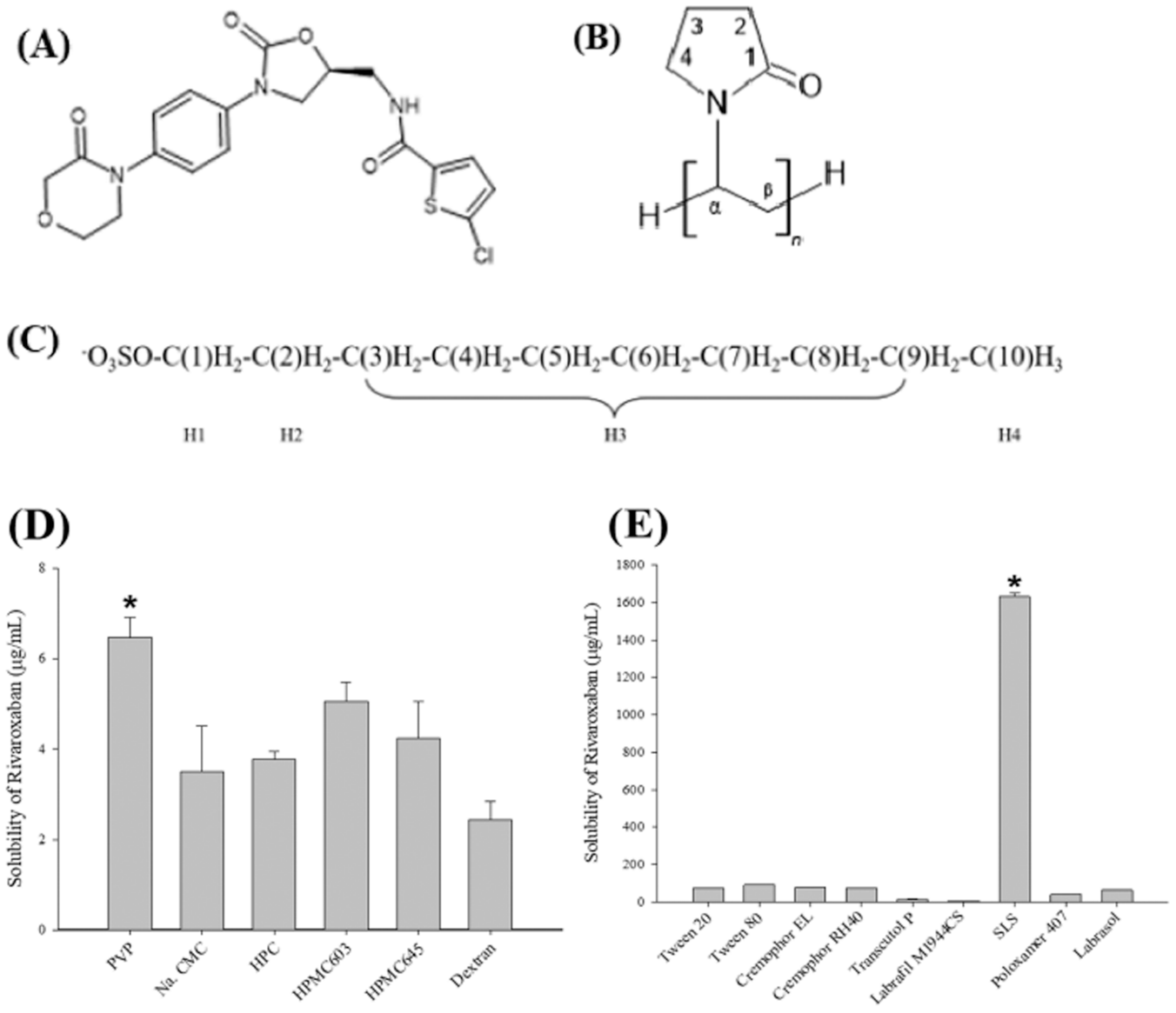

Figure 1. Chemical structure of rivaroxaban (A), PVP (B), SLS (C), and Drug solubility tests in (D) 1% polymer and (E) 10% surfactant solution. Each value represents the mean ± S.D. (n = 3). * means $p < 0.05$ compared to others.

(Shimadzu, Tokyo, Japan) and Shimadzu LCMS 8050 triple quadrupole mass spectrometer equipped with a C18 column (Phenomenex Luna column, 2.0 × 150 mm^2, 5 μm) in the positive ion mode. The supernatant was analyzed using a system with spray ionization.[22] The column temperature was maintained at 40 °C. The mobile phase consisted of a 45% (v/v) aqueous solution of acetonitrile containing 0.1% (v/v) formic acid and was used at a flow rate of 0.25 mL/min. All pharmacokinetic parameters were calculated using the non-compartmental analysis module (Certara USA, Inc., Princeton, NJ).[32]

2.7. Statistical Analysis. Data of the aqueous solubility and dissolution parameters were analyzed using one-way analysis of variance (ANOVA). Each value is represented as mean ± standard deviation (n = 3), and differences were considered statistically significant at *$p < 0.05$.[33]

3. RESULTS AND DISCUSSION

3.1. Optimization of RXB-Loaded Microspheres. To determine the proper carrier for RXB (Figure 1A), hydrophilic polymers and surfactants were screened using a solubility test.[34] Among the carriers tested, PVP (Figure 1B; 6.462 ± 0.447 μg/mL) had the highest drug solubility, which was significantly higher ($p < 0.05$) than that of other carriers (Figure 1D).[24] Therefore, PVP was selected as the hydrophilic carrier in this formulation.[34] Among the surfactants tested, RXB exhibited the highest solubility in SLS (Figure 1C; 1629.898 ± 18.864 μg/mL), which was significantly higher ($p < 0.05$) than that in other surfactants (Figure 1E).[25] In this study, PVP and SLS were chosen as carriers in the RXB-loaded microsphere formulation for further studies because of their high drug solubility, good compatibility with the drug, and improved stability of drug in solid state and in solution. In addition, RXB-loaded microspheres were developed by a spray-drying technique using polymers and surfactants as carriers. Among the various solubilization strategies, polymeric microspheres have the following advantages: small particle size (range of 1−100 nm), large surface area, easy preparation technique, protection against unstable drugs before and after administration, and prevention of precipitation.[35]

https://doi.org/10.1021/acs.molpharmaceut.3c00281
Mol. Pharmaceutics 2023, 20, 4153−4164

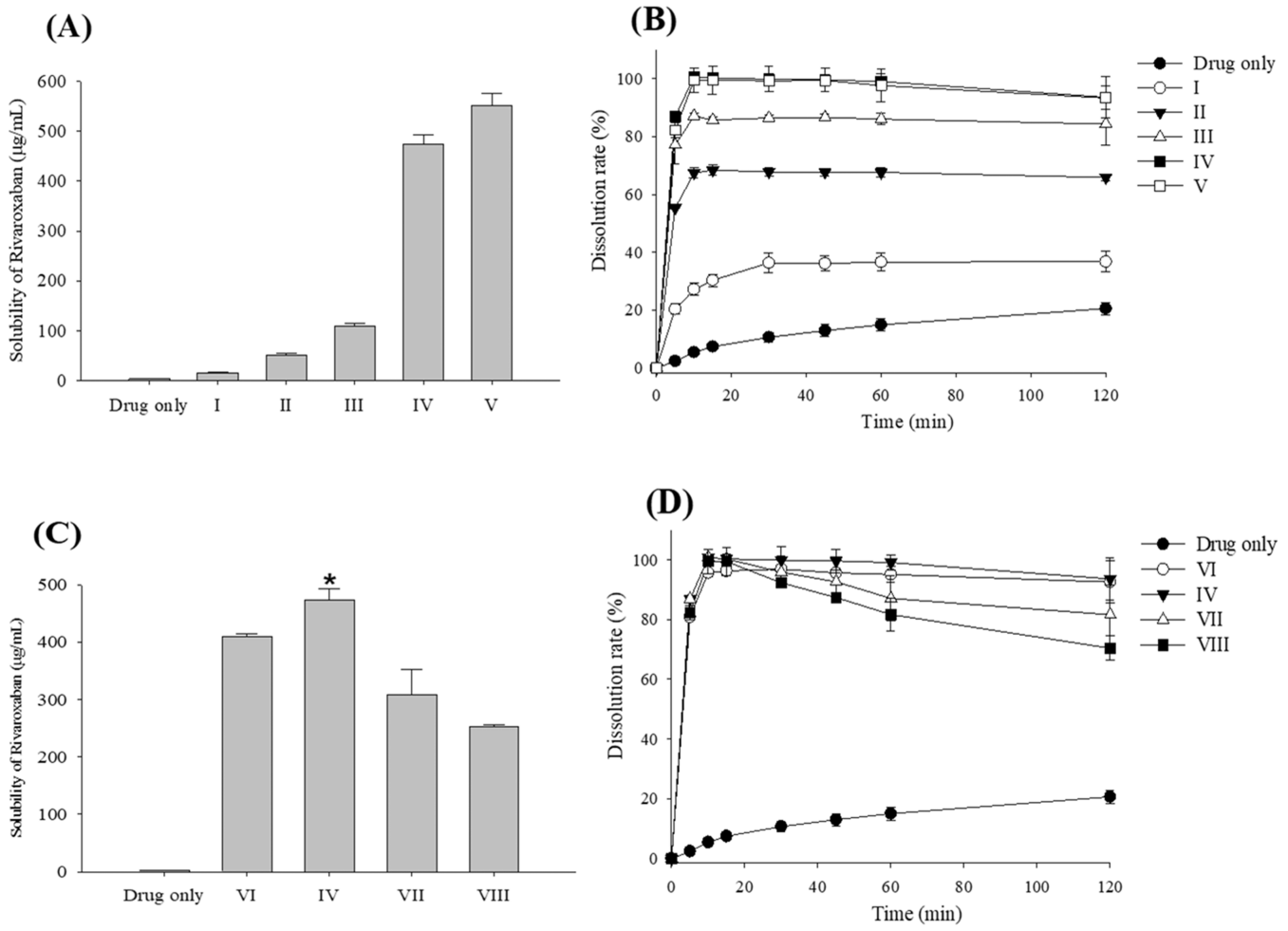

Figure 2. Effect of SLS amount on the solubility (A) and dissolution (B) of RXB-loaded microspheres. Effect of PVP amount on the solubility (C) and dissolution (D) of RXB-loaded microspheres. Each value represents the mean ± S.D. (n = 3). * means $p < 0.05$ compared to others.

Aqueous solubility and dissolution tests were carried out to optimize the ratio of the drug and carriers. To determine the optimal drug-carrier ratio, various formulations were prepared by fixing the concentration of the drug and altering the amount of carrier (Table 1). To study the effect of SLS on drug solubility and dissolution, the amount of RXB was fixed at 1 g and that of PVP at 0.25 g, and the amount of SLS was changed from 0.5 to 4 g (formulations I–V). We found that increasing the amount of SLS significantly increased ($p < 0.05$) the aqueous solubility of RXB (Figure 2A). However, when the amount of SLS was increased to 2 g, drug dissolution increased, but no significant difference ($p > 0.05$) was observed with further increases (Figure 2B). Therefore, 2 g SLS (formulation IV) was determined to be the appropriate amount of surfactant. Next, to examine the effect of PVP on drug solubility and dissolution, the amount of RXB was fixed to 1 g and that of SLS to 2 g, and then the amount of PVP was changed from 0.25 to 1 g (formulations IV and VI–VIII). It was found that the drug solubility was significantly the highest ($p < 0.05$) when the PVP amount was 0.25 g (Figure 2C), and the dissolution rate of RXB increased as the PVP amount decreased (Figure 2D). In general, the solubility of the drug increased as the amount of polymer carrier increased; however, in this study, a large amount of PVP decreased the solubility and dissolution rate of the drug. Although a large amount of polymer is required to molecularly dissolve the drug in solid dispersions, it is known that the use of large amounts of polymers causes problems such as limited drug loading, and the deliquescent nature of hydrophilic polymers causes phase separation and is physically unstable.[32] In this study, we observed that the final dissolution rate decreased owing to recrystallization and precipitation in the case of a formulation with a large amount of PVP (Figure 2D). These results suggest that large amounts of PVP caused phase separation, drug recrystallization, and physical destabilization of RXB-loaded microspheres.[36,37] The results of this study showed that a small amount of PVP was effective in increasing the dissolution rate of RXB to achieve better efficacy. Therefore, microspheres with a ratio of RXB, PVP, and SLS of 1/0.25/2 (formulation IV) were selected for further study based on their highest aqueous solubility and dissolution results.[38]

3.2. Characterizations of RXB-Loaded Microspheres.

3.2.1. Surface Morphology and Particle Size Distribution. Scanning electron microscopy was performed to obtain micrographs of RXB powder and optimized RXB-loaded microspheres and is widely used to investigate particle morphology.[38] The shape and surface morphology of RXB powder and selected RXB-loaded microspheres (formulations IV and VIII) were investigated and are shown in Figure 3A–F.[39] RXB appeared as irregular crystals with a smooth surface, whereas the RXB-loaded microspheres had spherical particles with a smooth surface.[40] This suggests that crystalline RXB was

https://doi.org/10.1021/acs.molpharmaceut.3c00281
Mol. Pharmaceutics 2023, 20, 4153–4164

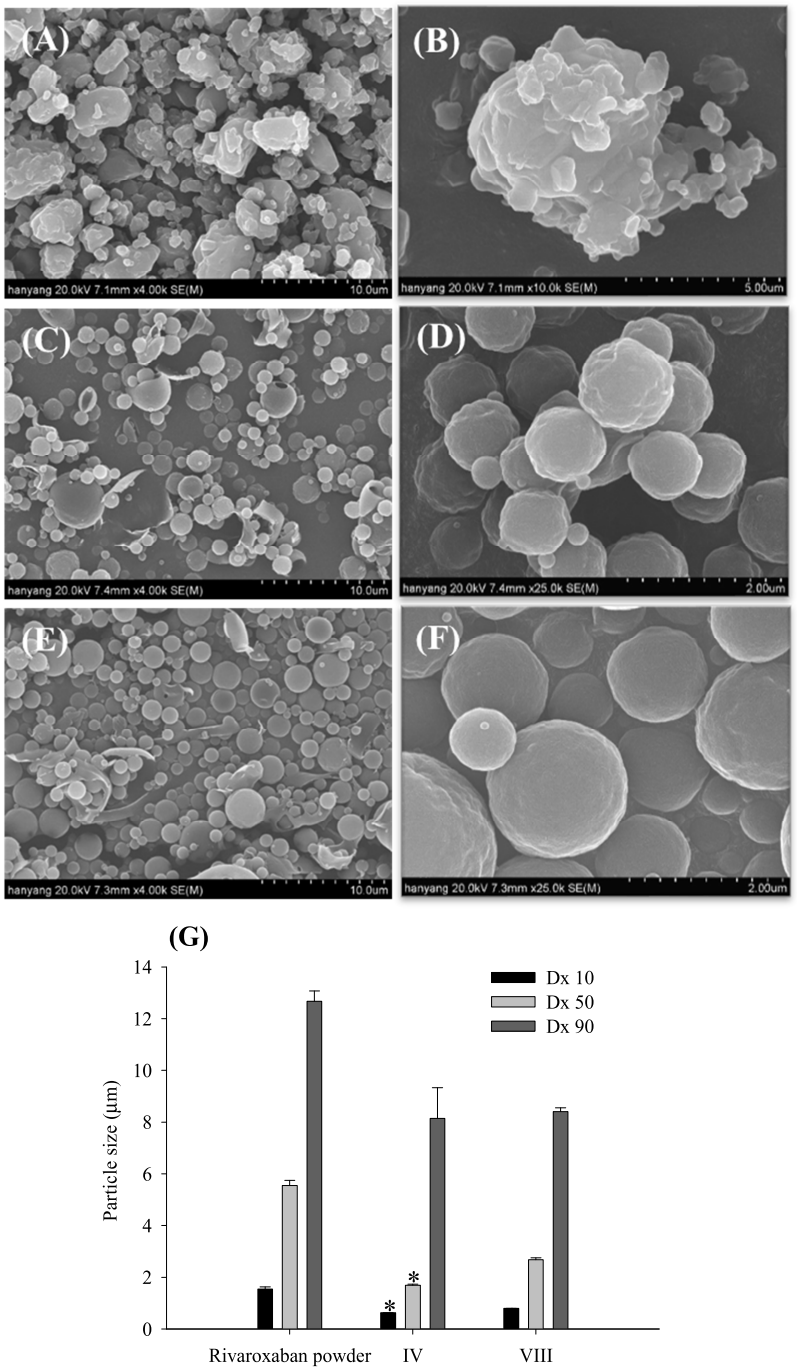

Figure 3. Scanning electron micrographs. (A) Rivaroxaban powder (×4000). (B) Rivaroxaban powder (×10,000). (C) Formulation IV (×4000). (D) Formulation IV (×25,000). (E) Formulation VIII (×4000). (F) Formulation VIII (×25,000) and (G) particle size distribution for drug powder, formulation IV, and formulation VIII. * means $p < 0.05$ compared to others.

converted to an amorphous form.[18] In addition, the reduced crystallinity of RXB in the microspheres was further confirmed by XRD and DSC results.[41]

The particle size distribution of the RXB-loaded microspheres prepared by spray drying is shown in Figure 3G.[28] Particle size and distribution of RXB powder and formulations IV and VIII were investigated. The mean diameter D50 was 5.55 ± 0.20 μm for RXB, and the mean diameters for formulation IV and VIII were 1.70 ± 0.04 and 2.68 ± 0.08 μm, respectively, which were significantly decreased compared to those for RXB powder ($p < 0.05$). In addition, the mean diameter D50 of formulation IV was significantly lower than that of formulation VIII ($p < 0.05$). Similar results were obtained for the distributions of D10 and D90. Thus, it is suggested that the improved solubility and bioavailability of the selected RXB-loaded microspheres were a result of their smaller particle size and narrow size distribution.[24]

3.2.2. Thermal Characteristics and Crystallinity. A PXRD study was conducted to confirm the crystallinity of pure RXB, RXB/PVP/SLS physical mixture, and selected RXB-loaded microspheres, as shown in Figure 4A. The sharp and intense peak in the XRD pattern of pure RXB (a) showed crystalline

https://doi.org/10.1021/acs.molpharmaceut.3c00281
Mol. Pharmaceutics 2023, 20, 4153−4164

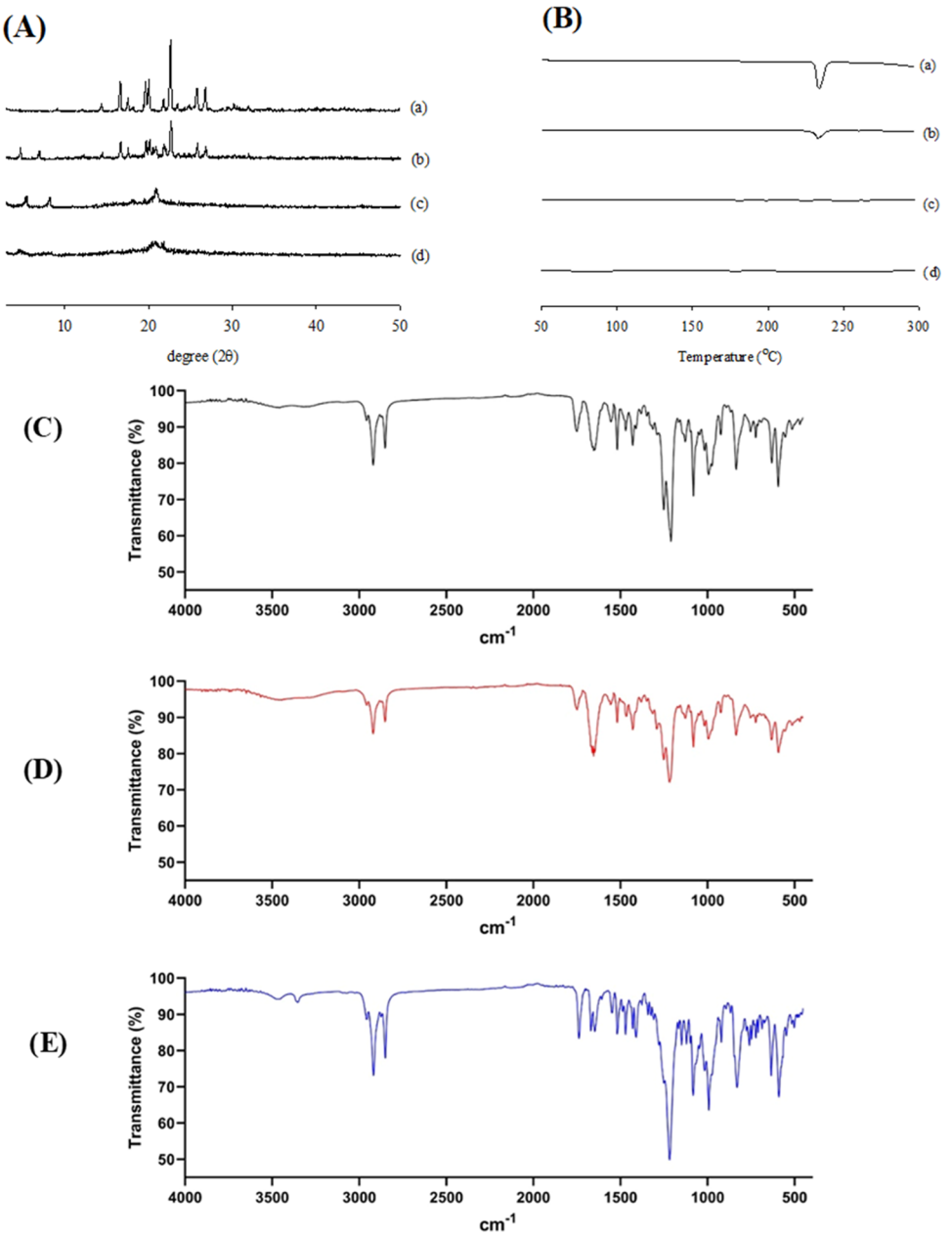

Figure 4. X-ray diffractometer (A) and differential scanning calorimetry thermogram (B) results for (a) rivaroxaban, (b) physical mixture, (c), formulation IV, and (d) formulation VIII. FTIR spectra for (C) formulation IV, (D) formulation VIII, and (E) physical mixture of formulation IV.

properties, whereas the physical mixture of RXB, PVP, and SLS showed a lower-intensity peak than the pure drug (b).[24] However, the XRD patterns of formulations IV and VIII (c and d) showed a halo pattern, and the crystalline peak of pure RXB peak disappeared. This suggests that the RXB-loaded microspheres (formulations IV and VIII) were converted from the crystalline to the amorphous form.[42]

The thermal characteristics of RXB powder, physical mixture, and microspheres are presented in Figure 4B. The DSC thermogram of RXB shows a sharp melting endotherm at approximately 230 °C, indicating its crystalline nature (a). A physical mixture was prepared by mixing RXB, PVP, and SLS, and a relatively weak peak corresponding to the drug was observed (b).[27] However, the sharp endothermic peak corresponding to the melting point of the drug disappeared in microsphere formulations IV and VIII, suggesting that the drug existed in an amorphous state (c and d).[43]

3.2.3. FTIR and ^{1}H NMR Spectroscopic Analysis. The interaction between RXB and the carrier was confirmed by comparing the FTIR spectra of the physical mixture (RXB/PVP/SLS = 1:0.25:2) and the RXB-loaded microspheres (formulations IV and VIII) (Figure 4C−E). The FTIR spectrum showed peaks in the range 450−4000 cm^{-1}. For the major peak of RXB, the corresponding functional group was identified with reference to the literature (−N−H− stretching: 3351.68 cm^{-1}; −N−C═O (carbamate) stretching: 1736.58 cm^{-1}; C═O (amide) stretching: 1668 and 1644 cm^{-1}; −C−O− stretching: 1119.48 cm^{-1}, aromatic C−H− bending: 827.31 cm^{-1}; and −C−Cl− stretching: 756.92 cm^{-1}).[3,44] When examining the physical mixture of formulation IV, there were two separate bands at 1668 and 1644 cm^{-1}

https://doi.org/10.1021/acs.molpharmaceut.3c00281
Mol. Pharmaceutics 2023, 20, 4153−4164

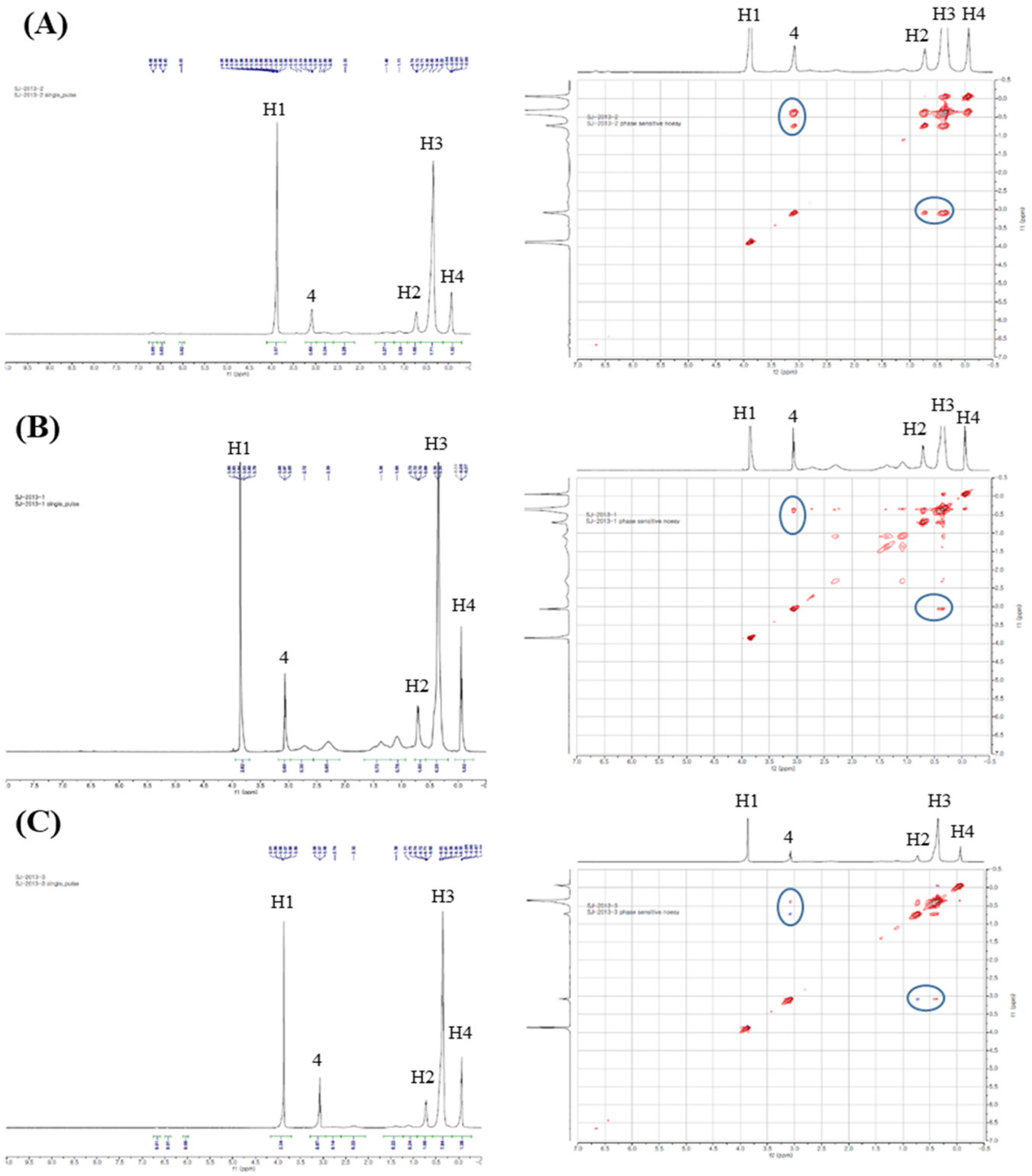

Figure 5. 1D ^{1}H NMR spectrum and contour plot of NOESY for (A) formulation IV, (B) formulation VIII, and (C) physical mixture of formulation IV. The assignments of protons are shown in Figure 1A−C.

corresponding to the C═O stretching of the amide group (Figure 4E). However, formulations IV and VIII showed relatively broad bands at 1655 cm^{-1} for amide group stretching, presumably owing to intermolecular interactions (e.g., hydrogen bonding) between RXB and PVP (Figure 4C−D). Intermolecular drug−excipient and excipient−excipient interactions are an important factor for physical safety to maintain a supersaturated state and inhibit crystallization of amorphous drugs. These results were further confirmed by the ^{1}H NMR results.

Based on the 1D ^{1}H NMR proton spectra, the cross peaks in 2D-NOESY connected spatially close resonances, providing clear signals for spatial packing and interactions between different functional groups in RXB, PVP, and SLS (Figure 5).

https://doi.org/10.1021/acs.molpharmaceut.3c00281
Mol. Pharmaceutics 2023, 20, 4153−4164

The proton peaks of PVP and SLS were assigned according to the literature.[45,46] In the PVP 1D ^{1}H NMR proton spectrum, the hydrogens in the polymer backbone are denoted by α and β, respectively, and the CH groups in the pyrrolidone ring are denoted by numbers (Figure 1B). In addition, the 1D ^{1}H NMR proton spectrum of SLS revealed four groups of signals, designated H1, H2, H3, and H4, as shown in Figure 1C. The 2D-NOESY spectra of formulation IV confirmed the presence of intermolecular interactions between the proton peak of PVP (position 4) and the H2 and H3 proton peaks of SLS (circled dots in Figure 5). However, in the NOESY spectrum of formulation VIII, there was no interaction between position 4 and H2 protons in the SLS because there were no cross peaks at the corresponding positions. This result suggested that formulation IV had a stronger hydrogen bond-type intermolecular interaction between PVP and SLS than formulation VIII.[21] This effect was attributed to polymer−surfactant interactions, which inhibited the reorganization of solute clusters and crystal growth, thereby maintaining RXB supersaturation.[47] In conclusion, NMR and FTIR spectroscopic analyses were successful in identifying differences in the intermolecular interactions of formulations IV and VIII, confirming that intermolecular interactions are important factors in inhibiting drug precipitation and increasing the solubilization of RXB.[44,48]

These physicochemical evaluations (SEM, DSC, PXRD, FTIR, and NMR) were useful for investigating polymer/surfactant interactions. The enhancement of solubility and stability in the amorphous state due to polymer and surfactant interactions is drug-dependent, and the excipients used for RXB-loaded microspheres may not exhibit the same behavior for different compounds. However, formulation design through polymeric/surfactant compatibility evaluation is essential for improving the solubility of drugs and stability of amorphous states.[21,47]

3.3. Pharmacokinetic Studies. The pharmacokinetic parameters of RXB were obtained after the oral administration of pure RXB powder and selected microspheres (formulations IV and VIII). Formulation IV, the selected RXB-loaded microspheres, consisted of RXB/PVP/SLS at a weight ratio of 1:0.25:2, whereas formulation VIII had a RXB/PVP/SLS weight ratio of 1:1:2.[26] Figure 6 shows the mean plasma concentration profile of RXB after oral administration of RXB powder and selected RXB microspheres (formulations IV and VIII) at a dose of 10 mg/kg.[19] The microsphere formulations had higher plasma concentrations of RXB at each time point than RXB powder. At every time point (except 24 h), the plasma concentrations of RXB after the administration of the microsphere formulations were significantly higher than those after the administration of RXB powder ($p < 0.05$).[31]

The pharmacokinetic parameters are presented in Table 2. The selected microsphere formulations (IV and VIII) had a significantly higher AUC (Area under the curve) and C_{max} (Maximum concentration of a drug achieved after dosing) than RXB powder ($p < 0.05$). Formulation IV provided significantly higher AUC values than formulation VIII ($p < 0.05$). However, other parameters, such as T_{max} (time to maximum plasma concentration), $t_{1/2}$ (half-life), and K_{el} (elimination rate constant) values, were not significantly different between the microsphere formulations (IV and VIII) and RXB powder.[24] Formulations IV and VIII provided approximately 2.4-fold and 1.7-fold higher AUC for the drug compared to RXB powder, respectively, and improved C_{max} by 2.5- and 2-fold, respectively, compared to RXB powder. This suggests that the enhanced oral bioavailability of RXB, a poorly soluble drug, in microspheres is due to a significant increase in the initial dissolution and absorption of RXB from the microsphere formulation.[25] Consequently, the obtained pharmacokinetic profiles and parameters significantly improved the bioavailability of the selected RXB-loaded microspheres compared to that of pure RXB powder.[49] These results demonstrated that the synergistic effect of the optimal PVP and SLS ratio combination improved the solubility and dissolution rate of RXB, a poorly soluble drug, which ultimately improved its bioavailability.[50]

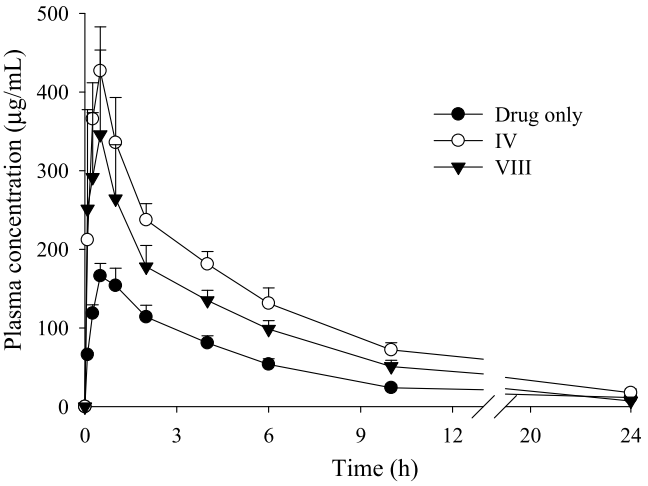

Figure 6. Plasma concentration−time curves for the drug only and RXB-loaded microspheres following oral administration in rats. Formulation IV was composed of RXB/PVP/SLS (1:0.25:2, w/w). Formulation VII was composed of RXB/PVP/SLS (1:1:2, w/w). Each value represents the mean ± S.D. ($n = 6$).

Table 2. Pharmacokinetic Parameters[a]

parameters	drug powder	IV	VIII
AUC (h·μg/mL)	1002.0 ± 82.3	2400.8 ± 237.1[c]	1761.4 ± 137.0[b]
C_{max} (μg/mL)	166.1 ± 15.9	427.0 ± 55.8[b]	345.9 ± 107.6[b]
T_{max} (h)	0.5 ± 0.0	0.5 ± 0.0	0.5 ± 0.0
$t_{1/2}$ (h)	0.11 ± 0.01	0.11 ± 0.01	0.13 ± 0.03
K_{el} (h^{-1})	6.05 ± 0.41	6.38 ± 0.81	5.23 ± 0.54

[a]Each value represents the mean ± S.D. ($n = 6$). [b]$p < 0.05$, compared to the drug powder. [c]$p < 0.05$, compared to the drug powder and formulation VIII.

4. CONCLUSIONS

In this study, we confirmed that intermolecular interactions between drugs, polymers, and surfactants led to different solubilities and the maintenance of amorphous stability. To develop optimal microspheres, it is important to find optimal ratios of drugs, polymers, and surfactants and to explore their intermolecular interactions. The developed microspheres consisting of RXB, PVP, and SLS were prepared in optimized proportions (1:0.25:2) using a spray-drying method, which significantly improved the drug solubility, solubility, and oral bioavailability. The selected microsphere formulation enhanced the solubility and dissolution rate by converting the drug from a crystalline to an amorphous form and reducing the particle size using the solvent evaporative spray-drying method. To maximize the oral bioavailability of RXB, a poorly soluble

https://doi.org/10.1021/acs.molpharmaceut.3c00281
Mol. Pharmaceutics 2023, 20, 4153−4164

drug, we investigated the interactions between drugs, polymers, and surfactants and developed optimal RXB-loaded microsphere formulations. Our results showed that the optimized microspheres loaded with RXB had significantly higher AUC and C_{max} values than pure RXB powder, indicating that the oral bioavailability of RXB could be improved in rats. In solubility, in vitro dissolution, and oral bioavailability studies, the developed RXB-loaded microspheres exhibited improved solubility and bioavailability compared with pure RXB powder. These results can be explained by the synergistic effect of the combination of PVP and SLS as well as the intermolecular interaction between the drug and excipient. Therefore, our studies proved that the newly developed RXB-loaded microspheres are promising as an improved oral drug delivery system for the poorly soluble drug RXB.

AUTHOR INFORMATION

Corresponding Authors

Han-Gon Choi − *College of Pharmacy, Hanyang University, Ansan 15588, South Korea*; Phone: +82-31-400-5802; Email: hangon@hanyang.ac.kr; Fax: +82-31-400-5958

Sung Giu Jin − *Department of Pharmaceutical Engineering, Dankook University, Cheonan 31116, South Korea*; orcid.org/0000-0003-1558-5155; Phone: +82-41-550-3558; Email: sklover777@dankook.ac.kr; Fax: +82-41-559-7945

Authors

Min-Jong Choi − *Department of Pharmaceutical Engineering, Dankook University, Cheonan 31116, South Korea*

Mi Ran Woo − *College of Pharmacy, Hanyang University, Ansan 15588, South Korea*

Kyungho Baek − *Department of Pharmaceutical Engineering, Dankook University, Cheonan 31116, South Korea*

Ji Hun Park − *Department of Science Education, Ewha Womans University, Seoul 03760, South Korea*; orcid.org/0000-0001-8218-0823

Seewon Joung − *Department of Chemistry, Inha University, Incheon 22212, South Korea*; orcid.org/0000-0002-6989-444X

Yong Seok Choi − *College of Pharmacy, Dankook University, Cheonan 31116, South Korea*

Complete contact information is available at: https://pubs.acs.org/10.1021/acs.molpharmaceut.3c00281

Author Contributions

#M.-J.C. and M.R.W. contributed equally to this work.

Notes

The authors declare no competing financial interest.

ACKNOWLEDGMENTS

This work was financially supported by a National Research Foundation of South Korea (NRF) grant funded by the South Korean government (MEST) (No. 2022R1A2C2004197) and the Basic Science Research Program through the National Research Foundation of Korea (NRF) funded by the Ministry of Education (NRF-2020R1A6A1A03043283). This research was supported by Korea Basic Science Institute (National Research Facilities and Equipment Center) grant funded by the Ministry of Education (Grant No. 2019R1A6C1010033).

REFERENCES

(1) Abouhussein, D. M. N.; Mahmoud, D. B. E. D.; F, E. M. Design of a liquid nano-sized drug delivery system with enhanced solubility of rivaroxaban for venous thromboembolism management in paediatric patients and emergency cases. *J. Liposome Res.* **2019**, *29*, No. 399.

(2) Hanafy, A. S.; Abd-Elsalam, S.; Dawoud, M. M. Randomized controlled trial of rivaroxaban versus warfarin in the management of acute non-neoplastic portal vein thrombosis. *Vascul. Pharmacol.* **2019**, *113*, 86−91.

(3) Bonaca, M. P.; Bauersachs, R. M.; Anand, S. S.; Debus, E. S.; Nehler, M. R.; Patel, M. R.; Fanelli, F.; Capell, W. H.; Diao, L.; Jaeger, N.; Hess, C. N.; Pap, A. F.; Kittelson, J. M.; Gudz, I.; Lajos Mátyás, L.; Krievins, D. K.; Diaz, R.; Brodmann, M.; Muehlhofer, E.; Lloyd, P. H.; Berkowitz, S. D.; Hiatt, W. R. Rivaroxaban in peripheral artery disease after revascularization. *N. Engl. J. Med.* **2020**, *382*, 1994−2004.

(4) Metre, S.; Mukesh, S.; Samal, S. K.; Chand, M.; Sangamwar, A. T. Enhanced biopharmaceutical performance of rivaroxaban through polymeric amorphous solid dispersion. *Mol. Pharm.* **2018**, *15*, 652−668.

(5) Hriňová, E.; Skořepová, E.; Čerňa, I.; Královičová, J.; Kozlík, P.; Křížek, T.; Roušarová, J.; Ryšánek, P.; Šíma, M.; Slanař, O. Explaining dissolution properties of rivaroxaban cocrystals. *Int. J. Pharm.* **2022**, *622*, No. 121854.

(6) Xue, X.; Cao, M.; Ren, L.; Qian, Y.; Chen, G. Preparation and Optimization of Rivaroxaban by Self-Nanoemulsifying Drug Delivery System (SNEDDS) for Enhanced Oral Bioavailability and No Food Effect. *AAPS PharmSciTech* **2018**, *19*, 1847−1859.

(7) Sherje, A. P.; Jadhav, M. *β*-Cyclodextrin-based inclusion complexes and nanocomposites of rivaroxaban for solubility enhancement. *J. Mater. Sci. Mater. Med.* **2018**, *29*, No. 186.

(8) Lee, J. H.; Jeong, H. S.; Jeong, J. W.; Koo, T. S.; Kim, D. K.; Cho, Y. H.; Lee, G. W. The development and optimization of hot-melt extruded amorphous solid dispersions containing Rivaroxaban in combination with polymers. *Pharmaceutics* **2021**, *13*, No. 344.

(9) Anwer, M. K.; Mohammad, M.; Iqbal, M.; Ansari, M. N.; Ezzeldin, E.; Fatima, F.; Alshahrani, S. M.; Aldawsari, M. F.; Alalaiwe, A.; Alzahrani, A. A.; Aldayel, A. M. Sustained release and enhanced oral bioavailability of rivaroxaban by PLGA nanoparticles with no food effect. *J. Thromb. Thrombolysis.* **2020**, *49*, 404−412.

(10) Zhang, X.; Xing, H.; Zhao, Y.; Ma, Z. Pharmaceutical dispersion techniques for dissolution and bioavailability enhancement of poorly water-soluble drugs. *Pharmaceutics* **2018**, *10*, No. 74.

(11) Everaerts, M.; Cools, L.; Adriaensens, P.; Reekmans, G.; Baatsen, P.; Van den Mooter, G. Investigating the Potential of Ethyl Cellulose and a Porosity-Increasing Agent as a Carrier System for the Formulation of Amorphous Solid Dispersions. *Mol. Pharm.* **2022**, *19*, 2712−2724.

(12) Frank, D. S.; Matzger, A. J. Probing the Interplay between Amorphous Solid Dispersion Stability and Polymer Functionality. *Mol. Pharm.* **2018**, *15*, 2714−2720.

(13) Pas, T.; Vergauwen, B.; Mooter, G. V. Exploring the feasibility of the use of biopolymers as a carrier in the formulation of amorphous solid dispersions − Part I: Gelatin. *Int. J. Pharm.* **2018**, *535*, 47−58.

(14) Choi, J. S.; Lee, S. E.; Jang, W. S.; Byeon, J. C.; Park, J. S. Solid dispersion of dutasteride using the solvent evaporation method: Approaches to improve dissolution rate and oral bioavailability in rats. *Mater. Sci. Eng. C* **2018**, *90*, 387−396.

(15) Saraf, I.; Roskar, R.; Modhave, D.; Brunsteiner, M.; Karn, A.; Neshchadin, D.; Gescheidt, G.; Paudel, A. Forced Solid-State Oxidation Studies of Nifedipine-PVP Amorphous Solid Dispersion. *Mol. Pharm.* **2022**, *19*, 568−583.

(16) Alizadeh, M. N.; Shayanfar, A.; Jouyban, A.; Ezzeldin, E. Solubilization of drugs using sodium lauryl sulfate: Experimental data and modelling. *J. Mol. Liq.* **2018**, *268*, 410−414.

(17) Yang, B.; Wu, L.; Ke, J.; Zhou, L.; Chen, M.; Li, S.; Feng, X. Effects of polymer/surfactant as carriers on the solubility and dissolution of fenofibrate solid dispersion. *AAPS PharmSciTech* **2019**, *20*, No. 102.

(18) Ko, D. W.; Cho, J. H.; Choi, H. G. Development of rebamipide-loaded spray-dried microsphere using distilled water and meglumine: physicochemical characterization and pharmacokinetics in rats. *Pharm. Dev. Technol.* **2021**, *26*, 701−708.
(19) Li, N.; Cape, J. L.; Mankani, B. R.; Zemlyanov, D. Y.; Shepard, K. B.; Morgen, M. M.; Taylor, L. S. Water-induced phase separation of spray-dried amorphous solid dispersions. *Mol. Pharm.* **2020**, *17*, 4004−4017.
(20) Pugliese, A.; Tobyn, M.; Hawarden, L. E.; Abraham, A.; Blanc, F. New Development in Understanding Drug−Polymer Interactions in Pharmaceutical Amorphous Solid Dispersions from Solid-State Nuclear Magnetic Resonance. *Mol. Pharm.* **2022**, *19*, 3685−3699.
(21) Liu, C.; Chen, Z.; Chen, Y.; Lu, J.; Li, Y.; Wang, S.; Wu, G.; Qian, F. Improving Oral Bioavailability of Sorafenib by Optimizing the "Spring" and "Parachute" Based on Molecular Interaction Mechanisms. *Mol. Pharm.* **2016**, *13*, 599−608.
(22) Choi, M. J.; Kim, J. S.; Yu, H. S.; Woo, M. R.; Choi, J. E.; Baek, K. H.; Kim, J. O.; Choi, Y. S.; Choi, H. G.; Jin, S. G. Comparison of the physicochemical properties, aqueous solubility, and oral bioavailability of RXB-loaded high-pressure homogenised and Shirasu porous glass membrane emulsified solid self-nanoemulsifying drug delivery systems. *J. Mol. Liq.* **2021**, *346*, No. 117057.
(23) Kim, D. S.; Cho, J. H.; Park, J. H.; Kim, J. S.; Song, E. S.; Kwon, J. W.; Giri, B. P.; Jin, S. G.; Kim, K. S.; Choi, H. G.; Kim, D. W. Self-microemulsifying drug delivery system (SMEDDS) for improved oral delivery and photostability of methotrexate. *Int. J. Nanomed.* **2019**, *14*, 4949−4960.
(24) Pandi, P.; Bulusu, R.; Kommineni, N.; Khan, W.; Singh, M. Amorphous solid dispersions: An update for preparation, characterization, mechanism on bioavailability, stability, regulatory considerations and marketed products. *Int. J. Pharm.* **2020**, *586*, No. 119560.
(25) Kim, J. S.; Park, J. H.; Jeong, S. C.; Kim, D. S.; Yousaf, A. M.; Din, F. U.; Kim, J. O.; Yong, C. S.; Youn, Y. S.; Oh, K. T.; Jin, S. G.; Choi, H. G. Novel revaprazan-loaded gelatin microsphere with enhanced drug solubility and oral bioavailability. *J. Microencapsulation* **2018**, *35*, 421−427.
(26) Choi, J. E.; Kim, J. S.; Kim, J.; Choi, M. J.; Baek, K.; Kim, J. O.; Choi, H. G.; Jin, S. G. A novel acidic microenvironment microsphere for enhanced bioavailability of carvedilol: Comparison of solvent evaporated and surface-attached system. *J. Drug Delivery Sci. Technol.* **2022**, *76*, No. 103803.
(27) Kim, J. S.; Din, F. U.; Lee, S. M.; Kim, D. S.; Woo, M. R.; Cheon, S. H.; Ji, S. H.; Kim, J. O.; Youn, Y. S.; Oh, K. T.; Lim, S. J.; Jin, S. G.; Choi, H. G. Comparison of Three Different Aqueous Microenvironments for Enhancing Oral Bioavailability of Sildenafil: Solid Self-Nanoemulsifying Drug Delivery System, Amorphous Microspheres and Crystalline Microspheres. *Int. J. Nanomed.* **2021**, *16*, 5797−5810.
(28) Sugamura, Y.; Fuji, M.; Nakanishi, S.; Suzuki, A.; Shibata, Y.; Koizumi, N.; Watanabe, Y. Effect of particle size of drug on conversion of crystals to an amorphous state in a solid dispersion with crospovidone. *Chem. Pharm. Bull.* **2011**, *59*, 235−238.
(29) Kim, J. S.; Choi, Y. G.; Woo, M. R.; Cheon, S. H.; Ji, S. H.; Im, D. S.; Din, F. U.; Kim, J. O.; Oh, K. T.; Lim, S. J.; Jin, S. G.; Choi, H. G. New potential application of hydroxypropyl-β-cyclodextrin in solid self-nanoemulsifying drug delivery system and solid dispersion. *Carbohydr. Polym.* **2021**, *271*, No. 118433.
(30) Han, J.; Tong, M.; Li, S.; Yu, X.; Hu, Z.; Zhang, Q.; Xu, R.; Wang, J. Surfactant-free amorphous solid dispersion with high dissolution for bioavailability enhancement of hydrophobic drugs: a case of quercetin. *Drug Dev. Ind. Pharm.* **2021**, *47*, 153−162.
(31) Kim, J. S.; Din, F. U.; Lee, S. M.; Kim, D. S.; Choi, Y. J.; Woo, M. R.; Kim, J. O.; Youn, Y. S.; Jin, S. G.; Choi, H. G. Comparative study between high-pressure homogenisation and Shirasu porous glass membrane technique in sildenafil base-loaded solid SNEDDS: Effects on physicochemical properties and in vivo characteristics. *Int. J. Pharm.* **2021**, *592*, No. 120039.
(32) Song, S.; Wang, C.; Wang, S.; Siegel, R. A.; Sun, C. C. Efficient development of sorafenib tablets with improved oral bioavailability enabled by coprecipitated amorphous solid dispersion. *Int. J. Pharm.* **2021**, *610*, No. 121216.
(33) Schver, G. C.; Nadvorny, D.; Lee, P. I. Evolution of supersaturation from amorphous solid dispersions in water-insoluble polymer carriers: Effects of swelling capacity and interplay between partition and diffusion. *Int. J. Pharm.* **2020**, *581*, No. 119292.
(34) Kim, S. J.; Lee, H. K.; Na, Y. G.; Bang, K. H.; Lee, H. J.; Wang, M.; Huh, H. W.; Cho, C. W. A novel composition of ticagrelor by solid dispersion technique for increasing solubility and intestinal permeability. *Int. J. Pharm.* **2019**, *555*, 11−18.
(35) Sur, S.; Rathore, A.; Dave, V.; Reddy, K. R.; Chouhan, R. S.; Sadhu, V. Recent developments in functionalized polymer nanoparticles for efficient drug delivery system. *Nano-Struct. Nano-Objects* **2019**, *20*, No. 100397.
(36) Nair, A. R.; Lakshman, Y. D.; Anand, V. S. K.; Sree, K. S. N.; Bhat, K.; Dengale, S. J. Overview of Extensively Employed Polymeric Carriers in Solid Dispersion Technology. *AAPS PharmSciTech* **2020**, *21*, No. 309.
(37) Kapourani, A.; Vardaka, E.; Katopodis, K.; Kachrimanis, K.; Barmpalexis, P. Rivaroxaban polymeric amorphous solid dispersions: moisture-induced thermodynamic phase behavior and intermolecular interactions. *Eur. J. Pharm. Biopharm.* **2019**, *145*, 98−112.
(38) Yousaf, A. M.; Malik, U. R.; Shahzad, Y.; Mahmood, T.; Hussain, T. Silymarin-laden PVP-PEG polymeric composite for enhanced aqueous solubility and dissolution rate: Preparation and in vitro characterization. *J. Pharm. Anal.* **2019**, *9*, 34−39.
(39) Mehenni, L.; Skiba, M. L.; Ladam, G.; Hallouard, F.; Skiba, M. Preparation and Characterization of Spherical Amorphous Solid Dispersion with Amphotericin B. *Pharmaceutics* **2018**, *10*, No. 235.
(40) Oo, M. K.; Mahmood, S.; Wui, W. T.; Mandal, U. K.; Chatterjee, B. Effects of different formulation methods on drug crystallinity, drug-carrier interaction, and ex vivo permeation of a ternary solid dispersion containing nisoldipine. *J. Pharm. Innovation* **2021**, *16*, 26−37.
(41) Choi, J. E.; Kim, J. S.; Choi, M. J.; Baek, K. H.; Woo, M. R.; Kim, J. O.; Choi, H. G.; Jin, S. G. Effects of different physicochemical characteristics and supersaturation principle of solidified SNEDDS and surface-modified microspheres on the bioavailability of carvedilol. *Int. J. Pharm.* **2021**, *597*, No. 120377.
(42) Yu, J. Y.; Kim, J. A.; Joung, H. J.; Ko, J. A.; Park, H. J. Preparation and characterization of curcumin solid dispersion using HPMC. *J. Food Sci.* **2020**, *85*, 3866−3873.
(43) Fan, W.; Zhu, W.; Zhang, X.; Xu, Y.; Di, L. Application of the combination of ball-milling and hot-melt extrusion in the development of an amorphous solid dispersion of a poorly water-soluble drug with high melting point. *RSC Adv.* **2019**, *9*, 22263−22273.
(44) Kini, A.; Patel, S. B. Phase behavior, intermolecular interaction, and solid state characterization of amorphous solid dispersion of Febuxostat. *Pharm. Dev. Technol.* **2017**, *22*, 45−57.
(45) Roehrig, S.; Straub, A.; Pohlmann, J.; Lampe, T.; Pernerstorfer, J.; Schlemmer, K. H.; Reinemer, P.; Perzborn, E. Discovery of the novel antithrombotic agent 5-chloro-N-({(5S)-2-oxo-3- [4-(3-oxo-morpholin-4-yl)phenyl]-1,3-oxazolidin-5-yl}methyl)thiophene- 2-carboxamide (BAY 59-7939): an oral, direct factor Xa inhibitor. *J. Med. Chem.* **2005**, *48*, 5900−5908.
(46) Roscigno, P.; Asaro, F.; Pellizer, G.; Ortona, O.; Paduano, L. Complex formation between poly(vinylpyrrolidone) and sodium decyl sulfate studied through NMR. *Langmuir* **2003**, *19*, 9638−9644.
(47) Deshpande, T. M.; Shi, H.; Pietryka, J.; Hoag, S. W.; Medek, A. Investigation of Polymer/Surfactant Interactions and Their Impact on Itraconazole Solubility and Precipitation Kinetics for Developing Spray-Dried Amorphous Solid Dispersions. *Mol. Pharm.* **2018**, *15*, 962−974.
(48) Pawar, J.; Suryawanshi, D.; Moravkar, K.; Aware, R.; Shetty, V.; Maniruzzaman, M.; Amin, P. Study the influence of formulation process parameters on solubility and dissolution enhancement of efavirenz solid solutions prepared by hot-melt extrusion: a QbD methodology. *Drug. Deliv. Transl.* **2018**, *8*, 1644−1657.

https://doi.org/10.1021/acs.molpharmaceut.3c00281
Mol. Pharmaceutics 2023, 20, 4153−4164

(49) Choi, J. S.; Cho, N. H.; Kim, D. H.; Park, J. S. Comparison of paclitaxel solid dispersion and polymeric micelles for improved oral bioavailability and in vitro anti-cancer effects. *Mater. Sci. Eng. C* **2019**, *100*, 247−259.
(50) Shi, X.; Xu, T.; Huang, W.; Fan, B.; Sheng, X. Stability and bioavailability enhancement of telmisartan ternary solid dispersions: the synergistic effect of polymers and drug-polymer(s) interactions. *AAPS PharmSciTech* **2019**, *20*, No. 143.

https://doi.org/10.1021/acs.molpharmaceut.3c00281
Mol. Pharmaceutics 2023, 20, 4153−4164